Synthesis, Structure, and Reactivity of $[RuCl(PP)L]PF_6$ (PP = $(PPh_3)_2$, $Ph_2P(CH_2)_4PPh_2$; L = $P(py)_3$, $PPh(py)_2$, py = 2-pyridyl). The "Missing" *P,N,N′*-Coordination Mode for 2-Pyridylphosphines

Richard P. Schutte, Steven J. Rettig, Ajey M. Joshi, and Brian R. James*

Department of Chemistry, University of British Columbia, 2036 Main Mall, Vancouver, BC, Canada V6T 1Z1

Received July 3, 1997[⊗]

The complexes $[RuCl(PPh_3)_2(P,N,N'\text{-}PPh_{3-x}(py)_x)]PF_6$ (x = 2, **1b**; 3, **1c**; py = 2-pyridyl) were isolated from the reaction of $RuCl_2(PPh_3)_3$ with 1 equiv of $PPh_{3-x}(py)_x$ and NH_4PF_6 in acetone. Crystals of **1b** ($C_{52}H_{43}ClF_6N_2P_4Ru$) are monoclinic, a = 17.795(2), b = 11.375(4), and c = 23.343(2) Å, β = 97.012(8)°, Z = 4, space group $P2_1/c$; those for **1c** ($C_{51}H_{42}ClF_6N_3P_4Ru$) are monoclinic, a = 17.812(1), b = 11.353(2), and c = 23.391(1) Å, β = 97.738(5)°, Z = 4, space group $P2_1/c$. The isomorphous structures were solved by the Patterson method and were refined by full-matrix least-squares procedures to R = 0.036 and 0.033 (R_w = 0.035 and 0.031) for 7690 and 8121 reflections with $I \geq 3\sigma(I)$, respectively. The *P,N,N′*-coordination mode for 2-pyridylphosphines is previously unreported. The *P,N*-coordinated complexes *cis*-$RuCl_2(dppb)(PPh_{3-x}(py)_x)$ (x = 1−3; dppb = $Ph_2P(CH_2)_4PPh_2$) were made by isomerization of the corresponding *trans*-dichloro isomers, which are themselves synthesized from $RuCl_2(dppb)(PPh_3)$. The *cis* complexes in $CHCl_3$ or CH_2Cl_2 dissociate chloride reversibly with formation of *P,N,N′*-coordinated $PPh_{3-x}(py)_x$ species, which were isolated as $[RuCl(dppb)(PPh_{3-x}(py)_x)]PF_6$ (x = 2, 3). Reactions of CO with the species containing the strained *P,N,N′*-coordination mode lead to displacement of a coordinated pyridyl and formation of the *P,N*-coordinated complexes $[RuCl(CO)(PP)(PPh_{3-x}(py)_x)]PF_6$ (PP = $(PPh_3)_2$, x = 2, 3; and PP = dppb, x = 2, 3). The CO reactions are partially reversible. Solution structures of the complexes were determined by NMR, IR, and UV−visible spectroscopies and conductivity.

Introduction

The coordination chemistry of the 2-pyridylphosphines, $PPh_{3-x}(py)_x$ (x = 1−3; py = 2-pyridyl), has developed considerably in the past 25 years[1−6] and is of interest for the use of metal complexes in catalysis because of the different properties of coordinated P and N,[1] as well as for potential homogeneous catalysis in aqueous media.[2] In mononuclear complexes, these phosphines can bind with a variety of coordination modes: through the phosphorus only (*P*), the phosphorus and one pyridyl group (*P,N*), two pyridyl groups (*N,N′*; $PPh(py)_2$ and $P(py)_3$), three pyridyl groups (*N,N′,N″*; $P(py)_3$ only), and via the phosphorus and two pyridyl groups (*P,N,N′*; $PPh(py)_2$ and $P(py)_3$). Representative examples for each of these, except for the *P,N,N′*-mode, have appeared in the literature.[3−6] The *P,N,N′*-mode has been predicted, based on the idea that the larger covalent radius of P versus N would allow for other coordination modes (i.e., *P*; *P,N*; *P,N,N′*) compared to those of tris(2-pyridyl)amine ($N(py)_3$) where coordination does not involve the central amine nitrogen, because its lone pair of electrons is directed away from the pyridyl lone pairs.[6c]

Here we report on the synthesis, characterization, and reactivity of Ru(II) complexes containing *P,N,N′*-coordinated $PPh_{3-x}(py)_x$ (x = 2, 3) ligands. The X-ray crystal structures of $[RuCl(PPh_3)_2(P,N,N'\text{-}PPh_{3-x}(py)_x)]PF_6$ (x = 2, 3) are reported, along with synthesis of related 1,4-bis(diphenylphosphino)butane (dppb) systems.

Experimental Section

Materials and Instrumentation. All manipulations were carried out under Ar using standard Schlenk techniques. Solvents (Fisher or BDH) were dried and distilled under N_2 prior to use. NH_4PF_6 (Aldrich) was used as supplied. $RuCl_2(PPh_3)_3$,[7] $RuCl_2(dppb)(PPh_3)$,[8] and $PPh_2(py)$[3c] were prepared according to literature procedures. The syntheses of $PPh(py)_2$ and $P(py)_3$ were as described previously,[9] adapted from a literature procedure.[2c]

[⊗] Abstract published in *Advance ACS Abstracts,* November 1, 1997.

(1) (a) General review: Newkome, G. R. *Chem. Rev.* **1993**, *93*, 2067. (b) Carsares, J. P.; Espinet, P.; Hernando, R.; Itrube, G.; Villafane, F.; Ellis, D. D.; Orpen, A. G. *Inorg. Chem.*, **1997**, *36*, 44. (c) Drommi, D.; Nicolo, F.; Arena, C. G.; Bruno, G.; Faraone, F. *Inorg. Chim. Acta* **1994**, *221*, 109. (d) Gliadiali, S.; Pinna, L.;Arena, C. G.; Rotondo, E.; Faraone, *F. J. Mol. Catal.* **1991**, *66*, 183. (e) Abu-Gnim, C.; Amer, I. *J. Mol. Catal.* **1993**, *85*, L275.

(2) (a) Baird, I. R.; Smith, M. B.; James, B. R. *Inorg. Chim. Acta* **1995**, *235*, 291. (b) Xie, Y.; Lee, C.-L.; Yang, Y.; Rettig, S. J.; James, B. R. *Can. J. Chem.* **1992**, *70*, 751. (c) Kurtev, K.; Ribola, D.; Jones, R. A.; Cole-Hamilton, D. J.; Wilkinson, G. *J. Chem. Soc., Dalton Trans.* **1980**, 55.

(3) *P*-coordinated: (a) Lock, C. J. L.; Turner, M. A. *Acta Crystallogr., Sect. C* **1987**, *43*, 2096. (b) Farr, J. P.; Olmstead, M. M.; Wood, F. E.; Balch, A. L. *J. Am. Chem. Soc.* **1983**, *105*, 792. (c) Maisonnet, A.; Farr, J. P.; Olmstead, M. M.; Hunt, C. T.; Balch, A. L. *Inorg. Chem.* **1982**, *21*, 3961. (d) Farr, J. P.; Olmstead, M. M.; Balch, A. L. *J. Am. Chem. Soc.* **1980**, *102*, 6654.

(4) *P,N*-coordinated: (a) Olmstead, M. M.; Maisonnat, A.; Farr, J. P.; Balch, A. L. *Inorg. Chem.* **1981**, *20*, 4060. (b) See also: refs 1c and 2c.

(5) *N,N′*-coordinated: (a) Espinet, P.; Gómez-Elipe, P.; Villafañe, F. *J. Organomet. Chem.* **1993**, *450*, 145. (b) Ehrlich, M. G.; Fronczek, F. R.; Watkins, S. F.; Newkome, G. R.; Hager, D. C. *Acta Crystallogr., Sect. C* **1984**, *40*, 78.

(6) *N,N′,N″*-coordinated: (a) Gregorzik, R.; Wirbser, J.; Vahrenkamp, H. *Chem. Ber.* **1992**, *125*, 1575. (b) Keene, F. R.; Snow, M. R.; Stephenson, P. J.; Tiekink, E. R. T. *Inorg. Chem.* **1988**, *27*, 2040. (c) Boggess, R. K.; Zatko, D. A. *J. Coord. Chem.* **1975**, *4*, 217.

(7) Hallman, P. S.; Stephenson, T. A.; Wilkinson, G. *Inorg. Synth.* **1970**, *12*, 237.

(8) (a) Jung, C. W.; Garrou, P. E.; Hoffman, P. R.; Caulton, K. G. *Inorg. Chem.* **1984**, *23*, 726. (b) Joshi, A. M.; Thorburn, I. S.; Rettig, S. J.; James, B. R. *Inorg. Chim. Acta* **1992**, *198*−*200*, 283.

(9) (a) Reference 2b. (b) Xie, Y.; James, B. R. *J. Organomet. Chem.* **1991**, *417*, 277.

S0020-1669(97)00835-5 CCC: $14.00

NMR spectra were recorded at room temperature (~20 °C), unless stated otherwise, on a Varian XL-300 MHz (300 MHz for ^{1}H; 121.4 MHz for ^{31}P) spectrometer. ^{1}H shifts were recorded using the residual proton of the solvent as internal standard. All ^{31}P shifts were referenced to external 85% H_3PO_4. IR spectra were recorded on a Nicolet 5DX-FT spectrophotometer or a Mattson Genesis Series FTIR as Nujol mulls between KBr plates. UV−vis spectra were recorded on a Hewlett-Packard 8452A diode array spectrometer using quartz cells and are presented as λ_{max} or shoulder (sh) (nm)/ϵ_{max} (M^{-1} cm^{-1}). Conductivity measurements were made at 25 °C on freshly made 1.0 mM solutions of a complex in CH_3NO_2, using a Model RCM151B Serfass conductance bridge (A. H. Thomas Co. Ltd.) connected to a 3403 cell from the Yellow Springs Instrument Co. The cell constant was determined by measuring the resistance of an aqueous solution of KCl (0.0100 M, σ = 0.001 413 Ω^{-1} cm^{-1} at 25 °C).[10a] Molar conductivities (Λ_M) are given in units of Ω^{-1} mol^{-1} cm^2. The accepted range for 1:1 electrolytes under these conditions is 75−90.[10b] Elemental analyses were performed by Mr. P. Borda of this department.

In Situ Reaction of $RuCl_2(PPh_3)_3$ with 1 Equiv of $P(py)_3$. $RuCl_2(PPh_3)_3$ (0.017 g, 0.018 mmol) and $P(py)_3$ (0.005 g, 0.019 mmol) were put in a sealable 5 mm NMR tube. The tube was evacuated, and $CDCl_3$ was vacuum transferred into the tube, which was immersed in liquid N_2. The tube was then flame sealed and warmed to ~20 °C. The initially brown suspension formed a red solution after a few minutes. The ^{31}P{^{1}H} NMR spectrum was measured after 24 h and after 7 days; the resulting orange solution was then heated at 65 °C for 2 days and the spectrum remeasured.

$[RuCl(PPh_3)_2(PPh(py)_2)]PF_6$ (1b). A solution of $RuCl_2(PPh_3)_3$ (0.31 g, 0.33 mmol), $PPh(py)_2$ (0.087 g, 0.33 mmol), and NH_4PF_6 (0.054 g, 0.33 mmol) in acetone (20 mL) was stirred for 20 h at ~20 °C. The initially brown suspension became an orange, turbid solution that was filtered through Celite 545 along with acetone washings (10 mL). The filtrate volume was reduced (~5 mL), Et_2O (10 mL) was added, and the resulting solution was left overnight; X-ray quality red crystals were deposited. These were collected, washed with a 20% acetone/ether mixture (3 × 1 mL), and dried in air (0.16 g, 45%). UV−vis (CH_2Cl_2): 318(sh)/5390, 410/1710, 460(sh)/1160. Λ_M = 79.4. Anal. Calcd for $C_{52}H_{43}ClF_6N_2P_4Ru$: C, 58.35; H, 4.05; N, 2.62. Found: C, 58.15; H, 4.07; N, 2.55.

The filtrate was pumped to dryness to give a yellow, oily residue. Et_2O (10 mL) was added, and the resulting yellow precipitate was filtered, washed with Et_2O (2 × 5 mL), and then dried under vacuum (0.12 g). A ^{31}P{^{1}H} NMR ($CDCl_3$) spectrum of the precipitate showed peaks for **1b**, as well as several other signals: from δ 57 to 63 and −3 to −12 (36 peaks), major peaks; from δ 28 to 41 and −20 to −28 (25 peaks), minor peaks.

$[RuCl(PPh_3)_2(P(py)_3)]PF_6$ (1c). Acetone (40 mL) was added to a mixture of $RuCl_2(PPh_3)_3$ (0.51 g, 0.53 mmol), $P(py)_3$ (0.14 g, 0.53 mmol), and NH_4PF_6 (0.087 g, 0.53 mmol). The resulting red suspension was stirred for 20 h at ~20 °C. The final orange suspension was filtered through Celite 545 and the volume reduced (to ~10 mL). Ether (40 mL) was added to form an orange precipitate, which was filtered, washed with Et_2O (3 × 10 mL) and then acetone (2 × 1 mL), and dried under vacuum (0.22 g, 39%). UV−vis (CH_2Cl_2): 410(sh)/1520, 460(sh)/1110. Λ_M = 78.2. Anal. Calcd for $C_{51}H_{42}ClF_6N_3P_4Ru$: C, 57.18; H, 3.95; N, 3.92; Cl, 3.31. Found: C, 57.28; H, 3.93; N, 3.89; Cl, 3.12

A ^{31}P{^{1}H} NMR ($CDCl_3$) spectrum of the material isolated prior to the acetone wash showed peaks for **1c,** as well as a broad signal at δ 0 and two doublets at δ 61.4 and 2.64 ($^2J_{PP}$ = 34.5 Hz). These "impurities" occurred in small amounts and were removed by washing with acetone at the expense of the yield.

Single crystals of **1c** were grown by diffusion of ether into a CH_2Cl_2 solution of the complex.

***trans*-$RuCl_2(dppb)(PPh_2(py))$ (2a).** This compound was synthesized by a procedure corresponding to that described for **2b** (0.18 g, 91%). UV−vis (CH_2Cl_2): 346/2570. Anal. Calcd for $C_{45}H_{42}Cl_2NP_3Ru$: C, 62.72; H, 4.91; N,1.63; Cl, 8.23. Found: C, 62.59; H, 4.96; N, 1.51; Cl, 8.39.

***trans*-$RuCl_2(dppb)(PPh(py)_2)$ (2b).** A solution of $RuCl_2(dppb)(PPh_3)$ (0.20 g, 0.23 mmol) and $PPh(py)_2$ (0.06 g, 0.24 mmol) in benzene (15 mL) was stirred for 1.5 h. The initial green solution turned orange/brown. After the solution was stirred, the volume was reduced (to ~5 mL), and hexanes (30 mL) were added to form a light orange precipitate. After vacuum filtration, the precipitate was washed with hexanes (3 × 5 mL) to remove any residual PPh_3 and dried under vacuum (0.19 g, 93%). UV−vis (CH_2Cl_2): 342/2610. Anal. Calcd for $C_{44}H_{41}Cl_2N_2P_3Ru$: C, 61.26; H, 4.79; N, 3.25; Cl, 8.22. Found: C, 61.41; H, 5.03; N, 3.03; Cl, 8.07.

***trans*-$RuCl_2(dppb)(P(py)_3)$ (2c).** The title complex was synthesized by a procedure similar to that given for **2b** (0.17 g, 83%). UV−vis (CH_2Cl_2): 336/2710. Anal. Calcd for $C_{43}H_{40}Cl_2N_3P_3Ru$: C, 59.79; H, 4.67; N, 4.86; Cl, 8.21. Found: C, 60.03; H, 4.87; N, 4.82; Cl, 8.00.

***cis*-$RuCl_2(dppb)(PPh_2(py))$ (3a).** A solution of **2a** (0.12 g, 0.14 mmol) in benzene (10 mL) was refluxed for 1.5 h, over which time a yellow precipitate was deposited from the initially brown solution. Hexanes (30 mL) were added, and the precipitate was filtered and dried under vacuum (0.11 g, 91%). UV−vis (CH_2Cl_2): 338/2960. Λ_M = 66.7. Anal. Calcd for $C_{45}H_{42}Cl_2NP_3Ru$: C, 62.72; H, 4.91; N, 1.63; Cl, 8.23. Found: C, 62.36; H, 4.95; N, 1.65; Cl, 8.11.

***cis*-$RuCl_2(dppb)(PPh(py)_2)$ (3b).** A solution of **2b** (0.18 g, 0.20 mmol) in benzene (10 mL) was refluxed for 2 h. After 1.5 h, a yellow precipitate formed from the brown solution. The reaction mixture was concentrated (to ~7 mL) under vacuum, and hexanes (30 mL) were added to complete precipitation. The yellow product was filtered, washed with hexanes (2 × 10 mL), and dried under vacuum (0.16 g, 89%). UV−vis ($CHCl_3$): 320/4160. UV−vis (MeOH): 320/4970. Λ_M = 69.1. Anal. Calcd for $C_{44}H_{41}Cl_2N_2P_3Ru$: C, 61.26; H, 4.79; N, 3.25. Found: C, 61.30; H, 4.96; N, 3.08.

***cis*-$RuCl_2(dppb)(P(py)_3)$ (3c).** **3c** was prepared from **2c** (0.16 g, 93%) by the same procedure as for **3b**. UV−vis ($CHCl_3$): 320/4160. UV−vis (MeOH): 320/4970. Λ_M = 70.2. Anal. Calcd for $C_{43}H_{40}Cl_2N_3P_3Ru$: C, 59.79; H, 4.67; N, 4.86. Found: C, 59.69; H, 4.69; N, 4.76.

$[RuCl(dppb)(PPh(py)_2)]PF_6$ (4b). A suspension of **3b** (0.06 g, 0.07 mmol) in acetone (45 mL) was stirred for 15 min, and to the resulting clear solution was added NH_4PF_6 (0.01 g, 0.07 mmol); the cloudy reaction mixture was stirred for a further 1 h and then filtered through Celite 545. The yellow filtrate was concentrated (to ~3 mL), and ether (20 mL) followed by hexanes (10 mL) were added, causing formation of a yellow precipitate that was filtered, washed with hexanes (2 × 5 mL), and dried in vacuo (0.05 g, 82%). UV−vis ($CHCl_3$): 320/5100. UV−vis (MeOH): 320/5050. Λ_M = 79.4. Anal. Calcd for $C_{44}H_{41}ClF_6N_2P_4Ru$: C, 54.36; H, 4.25; N, 2.88; Cl 3.64. Found: C, 54.26; H, 4.32; N, 2.80; Cl, 3.81.

$[RuCl(dppb)(P(py)_3)]PF_6$ (4c). **4c** was prepared by the same procedure as for **4b**, but starting with **3c** (0.08 g, 0.093 mmol) (0.07g, 76%). UV−vis ($CHCl_3$): 320/5010. Λ_M = 81.2. Anal. Calcd for $C_{43}H_{40}ClF_6N_3P_4Ru\cdot H_2O$: C, 52.10; H, 4.27; N, 4.23. Found: C, 52.22; H, 4.42; N, 3.90. The presence of H_2O was confirmed in the ^{1}H NMR spectrum.

[*cis*-$RuCl(CO)(PPh_3)_2(PPh(py)_2)]PF_6$ (5b). To a Schlenk tube fitted with a rubber septum, and containing an orange solution of **1b** (0.050 g, 0.047 mmol) in acetone (1 mL), was added 1 equiv of CO gas (1.15 mL (1 atm), 0.047 mmol) via a gas-tight syringe. Over 4 h, the stirred solution turned yellow. After a further 20 h, ether (25 mL) was added; the off-white precipitate was collected and dried under vacuum (0.041 g, 80%). Anal. Calcd for $C_{53}H_{43}ClF_6N_2OP_4Ru$: C, 57.95; H, 3.94; N, 2.55. Found: C, 57.95; H, 4.07; N, 2.52.

[*cis*-$RuCl(CO)(PPh_3)_2(P(py)_3)]PF_6$ (5c). To a degassed solution of **1c** (0.16 g, 0.15 mmol) in CH_2Cl_2 or acetone (3 mL) was added CO gas (1 atm). The initially orange solution turned yellow after 5 min and was stirred for 1 h. The white product was precipitated with ether (20 mL), collected by filtration, and dried under vacuum (0.15 g, 91%). UV−vis (CH_2Cl_2): 268/14 200, 294/14 600. Λ_M = 78.8. Anal. Calcd for $C_{52}H_{42}ClF_6N_3OP_4Ru$: C, 56.81; H, 3.85; N, 3.82. Found: C, 56.47; H, 3.85; N, 3.74.

$[RuCl(CO)(dppb)(PPh_2(py))]PF_6$ (6a). To a degassed solution of **3a** (0.077 g, 0.090 mmol) and NH_4PF_6 (0.015 g, 0.093 mmol) in acetone

(10) (a) Lind, J. E. J.; Zwolenik, J. J.; Fuoss, R. M. *J. Am. Chem. Soc.* **1959**, *81*, 1557. (b) Geary, W. J. *Coord. Chem. Rev.* **1971**, *7*, 81.

Table 1. Crystallographic Data for $[RuCl(PPh_3)_2(PPh_{3-x}(py)_x)]PF_6$ ($x = 2$, **1b**; 3, **1c**)

	1b	**1c**
formula	$C_{52}H_{43}ClF_6N_2P_4Ru$	$C_{51}H_{42}ClF_6N_3P_4Ru$
fw	1070.33	1071.32
crystal system	monoclinic	monoclinic
space group	$P2_1/c$	$P2_1/c$
a, Å	17.795(2)	17.812(1)
b, Å	11.375(4)	11.353(2)
c, Å	23.343(2)	23.391(1)
β, deg	97.012(8)	97.738(5)
V, Å^3	4689(1)	4686(1)
Z	4	4
ρ_{calc}, g/cm^3	1.516	1.518
T, °C	21	21
radiation	Mo	Mo
λ, Å	0.710 69	0.710 69
μ, cm^{-1}	5.91	5.92
transmission factors	0.96−1.00	0.94−1.00
R (F)[a]	0.036	0.033
R_w (F)[a]	0.035	0.031

[a] $R = \sum||F_o| - |F_c||/\sum|F_o|$, $R_w = (\sum w(|F_o| - |F_c|)^2/\sum w|F_o|^2)^{1/2}$.

(5 mL) was added CO (1 atm). The resulting yellow suspension was stirred for 21 h, over which time a light yellow, turbid solution developed. The mixture was filtered through Celite 545 to remove NH_4Cl and concentrated (∼1 mL) under vacuum. Et_2O was added (20 mL), and the resulting lemon precipitate was filtered and dried under vacuum at 78 °C (0.064 g, 71%). Anal. Calcd for $C_{46}H_{42}ClF_6NOP_4Ru$: C, 55.29; H, 4.23; N, 1.40. Found: C, 55.64; H, 4.34; N, 1.40.

The product was a mixture of so-called *cis* (20%) and *trans′* (80%) complexes (see Discussion), based on integration of the dppb methylene signals in the ^{1}H NMR spectrum.

[*cis*-RuCl(CO)(dppb)(PPh$_{3-x}$(py)$_x$)]PF$_6$ ($x = 2$, *cis*-6b; 3, *cis*-6c). To a degassed solution of $[RuCl(dppb)(PPh_{3-x}(py)_x)]PF_6$ ($x = 2$, 0.06 g, 0.062 mmol; 3, 0.07 g, 0.072 mmol) in CH_2Cl_2 (3 mL) was added CO (1 atm). After the solution was stirred for 1 h, Et_2O (30 mL) was added, causing formation of a light yellow precipitate; this was collected and dried under vacuum (for $x = 2$, 0.05 g, 78%; for $x = 3$, 0.07 g, 94%).

Data for 6b. The Et_2O solvate was confirmed in the ^{1}H NMR ($CDCl_3$) spectrum (δ 1.20 (t) and 3.48 (q), $^2J_{HH} = 6.9$ Hz). Anal. Calcd for $C_{45}H_{41}ClF_6N_2OP_4Ru\cdot 0.5Et_2O$: C, 54.42; H, 4.47; N, 2.70. Found: C, 54.19; H, 4.36; N, 2.53.

Data for 6c. The Et_2O solvate was confirmed (see above). Anal. Calcd for $C_{44}H_{40}ClF_6N_3OP_4Ru\cdot 0.25Et_2O$: C, 52.39; H, 4.15; N, 4.07. Found: C, 52.37; H, 4.07; N, 4.06.

Isomerization of [*cis*-RuCl(CO)(dppb)(PPh$_{3-x}$(py)$_x$)]PF$_6$ ($x = 2$, 3) and CO Loss. Complex *cis*-**6b** or *cis*-**6c** (∼0.02−0.03 g) was placed in a 25 mL flask fitted with a condenser and attached to a vacuum line. The system was evacuated and put under Ar. $CHCl_3$ (5 mL) was added, and the resulting yellow solution was refluxed in the dark under Ar. After the refluxing procedure ($x = 2$, 16 h; $x = 3$, 24 h), the solvent was removed under vacuum, and the yellow-orange residue was analyzed by ^{31}P{^{1}H} and ^{1}H NMR ($CDCl_3$) and IR spectroscopies.

Isomerization of [*cis*-RuCl(CO)(dppb)(PPh$_{3-x}$(py)$_x$)]PF$_6$ ($x = 2$, 3). Complex *cis*-**6b** or *cis*-**6c** (∼0.05 g) was stirred in CH_2Cl_2 (2 mL) under CO (1 atm) at ∼20 °C. After 6 days, Et_2O (15 mL) was added, and the resulting precipitate was collected by filtration and analyzed by ^{31}P{^{1}H} and ^{1}H NMR ($CDCl_3$) and IR spectroscopies.

X-ray Crystallographic Analyses of 1b and 1c. Selected crystallographic data appear in Table 1. The final unit-cell parameters were obtained by least-squares methods on the setting angles for 25 reflections, with $2\theta = 25.1-30.3°$ for **1b** and 25.0−33.6° for **1c**. The intensities of three standard reflections, measured every 200 reflections throughout the data collections, decayed linearly by 5.7% for **1c** and remained constant for **1b**. The data were processed[11a] and corrected for Lorentz and polarization effects and absorption (empirical, based on azimuthal scans).

The isomorphous structures were solved by the Patterson method. All non-hydrogen atoms of both structures were refined with anisotropic thermal parameters. Hydrogen atoms were fixed in calculated positions (C−H = 0.98 Å, $B_H = 1.2\ B_{bonded\ atom}$). A correction for secondary extinction (Zacharaisen type) was applied for **1b**, the final value of the extinction coefficient being $7.4(4) \times 10^{-8}$. No secondary extinction correction was necessary for **1c**. Neutral atom scattering factors for all atoms[11b] and anomalous dispersion corrections for the non-hydrogen atoms[11c] were taken from the *International Tables for X-Ray Crystallography*. Selected bond lengths and bond angles appear in Table 2. A complete table of crystallographic data, final atomic coordinates and equivalent isotropic thermal parameters, anisotropic thermal parameters, bond lengths, bond angles, torsion angles, intermolecular contacts, and least-squares planes for both structures are included as Supporting Information.

Results and Discussion

For consistency in reading, **a**, **b**, or **c** refers specifically to complexes containing $PPh_{3-x}(py)_x$ ligands, with $x = 1$, 2, or 3, respectively.

Synthesis and Charaterization. Figure 1 summarizes the syntheses of the complexes. The observation of the *P,N,N′*-coordination mode stems from the in situ reaction of $RuCl_2(PPh_3)_3$ with 1 equiv of $P(py)_3$. The ^{31}P{^{1}H} NMR spectra of the in situ reaction mixture, after 24 h, showed several species; however, after 7 days the spectrum simplified to an A_2X pattern (*cis* $^2J_{AX}$)[12] and contained a singlet for free PPh_3 (−5.42 ppm). The A_2X pattern is associated with $[RuCl(PPh_3)_2(P,N,N'\text{-}P(py)_3)]Cl$ (**1c′**) for reasons which will become apparent. When the sample was then heated, the spectrum changed again, showing two singlets as well as the singlet for free PPh_3. The complex associated with the two singlets is $RuCl_2(PPh_3)(N,N',N''\text{-}P(py)_3)$ and has been described elsewhere.[13] On a synthetic scale in CH_2Cl_2 or $CHCl_3$, after 1 week at ∼20 °C, the same A_2X pattern for **1c′** was observed in the spectrum of the reaction mixture. After isolation by precipitation with ether or hexanes, the material obtained showed several different peaks in the ^{31}P-{^{1}H} NMR spectrum, leading to the conclusion that **1c′** was stable only when formed in situ. When this isolated material was refluxed in C_6H_6, $RuCl_2(PPh_3)(N,N',N''\text{-}P(py)_3)$ was isolated.

In order to improve the stability of compounds such as **1c′**, two approaches were taken. The first was to carry out the reaction in the presence of a large anion which would add stability if chloride dissociation was occurring, and the second was to use as starting material $RuCl_2(dppb)(PPh_3)$, which is similar to $RuCl_2(PPh_3)_3$ in its structure and chemistry,[8,14] and the chelating dppb ligand might add stability. Use of these two approches led to isolation of stable complexes with the *P,N,N′*-coordination mode.

The reaction of $RuCl_2(PPh_3)_3$ with 1 equiv of $PPh(py)_2$ or $P(py)_3$ in acetone in the presence of 1 equiv of NH_4PF_6 affords $[RuCl(PPh_3)_2(PPh_{3-x}(py)_x)]PF_6$ ($x = 2$ (**1b**), 3 (**1c**)), in 45% and 39% yields, respectively; other coproducts remain unidentified. The ^{31}P{^{1}H} NMR spectra of **1b** and **1c** (Table 3) consist of A_2X patterns with *cis* $^2J_{AX}$ coupling constants, as well as a

(11) (a) *teXsan: Crystal Structure Analysis Package*; Molecular Structure Corp.: The Woodlands, TX, 1985, 1992. (b) *International Tables for X-Ray Crystallography*, Vol. IV; Kynoch Press: Birmingham, England, 1974; pp 99−102. (c) International Tables for Crystallography, Vol. C; Kluwer Academic Publishers: Boston, MA, 1992; pp 200−206.
(12) Pregosin, P. W.; Kunz, R. W. *NMR* **1979**, *16*, 28.
(13) Schutte, R. P.; Rettig, S. J.; James, B. R. *Can. J. Chem.* **1996**, *74*, 2064.
(14) (a) Stephenson, T. A.; Wilkinson, G. *J. Inorg. Nucl. Chem.* **1966**, *28*, 945. (b) Hoffman, P. R.; Caulton, K. G. *J. Am. Chem. Soc.* **1975**, *97*, 4221.

Table 2. Selected Bond Lengths (Å) and Angles (deg) for $[RuCl(PPh_3)_2(PPh(py)_2)]PF_6$ (**1b**) and $[RuCl(PPh_3)_2(P(py)_3PF_6$ (**1c**), with Estimated Standard Deviations in Parentheses

	1b	1c		1b	1c
			Bonds		
Ru(1)−Cl(1)	2.4096(8)	2.4066(7)	P(1)−C(1)	1.821(3)	1.818(3)
Ru(1)−P(1)	2.2925(8)	2.2854(7)	P(1)−C(6)	1.825(3)	1.825(3)
Ru(1)−P(2)	2.3472(8)	2.3478(7)	P(1)−C(11)	1.797(3)	1.814(3)
Ru(1)−P(3)	2.3539(8)	2.3452(7)	N(1)−C(1)	1.359(4)	1.359(3)
Ru(1)−N(1)	2.161(2)	2.180(2)	N(2)−C(6)	1.361(4)	1.357(3)
Ru(1)−N(2)	2.180(2)	2.166(2)			
			Angles		
Cl(1)−Ru−P(1)	151.48(3)	151.59(3)	P(3)−Ru−N(2)	168.35(7)	167.30(6)
Cl(1)−Ru−P(2)	95.63(3)	94.16(3)	N(1)−Ru−N(2)	80.29(9)	80.07(7)
Cl(1)−Ru−P(3)	93.72(3)	96.20(3)	P(1)−C(1)−N(1)	100.8(2)	100.8(2)
Cl(1)−Ru−N(1)	90.71(7)	92.43(6)	P(1)−C(6)−N(2)	100.7(2)	100.8(2)
Cl(1)−Ru−N(2)	92.40(7)	90.75(6)	Ru−N(1)−C(1)	105.1(2)	104.6(2)
P(1)−Ru−P(2)	103.19(3)	103.16(3)	Ru−N(2)−C(6)	104.9(2)	104.9(2)
P(1)−Ru−P(3)	103.61(3)	102.47(2)	Ru−P(1)−C(1)	86.4(1)	87.02(8)
P(1)−Ru−N(1)	67.24(7)	66.95(6)	Ru−P(1)−C(6)	86.86(10)	86.45(9)
P(1)−Ru−N(2)	67.05(7)	67.35(6)	Ru−P(1)−C(11)	150.2(1)	151.87(9)
P(2)−Ru−P(3)	100.30(3)	100.46(3)	C(1)−P(1)−C(6)	96.1(1)	96.6(1)
P(2)−Ru−N(1)	167.74(7)	167.81(6)	C(1)−P(1)−C(11)	111.5(1)	110.9(1)
P(2)−Ru−N(2)	88.95(7)	89.59(6)	C(6)−P(1)−C(11)	113.3(1)	111.6(1)
P(3)−Ru−N(1)	89.72(7)	89.00(6)			

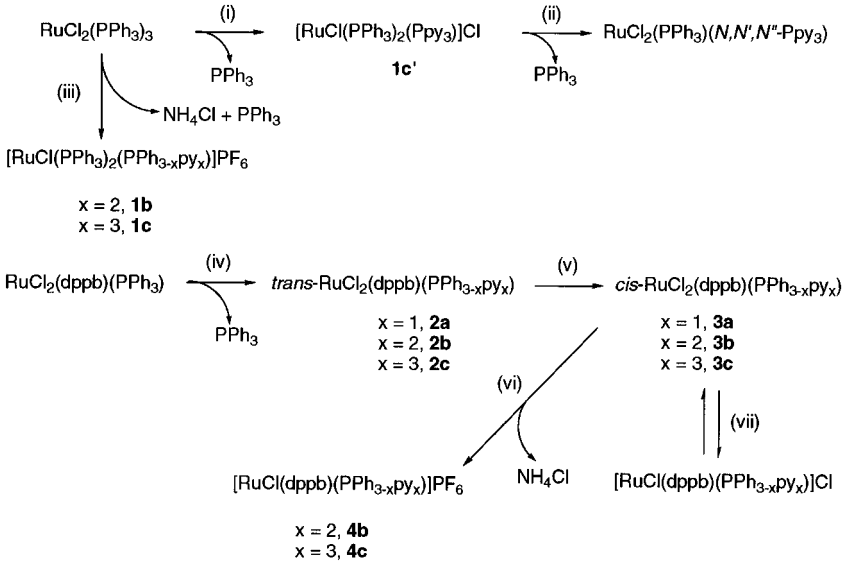

Figure 1. Summary of synthesis of compounds. Reaction conditions: (i) in situ, $P(py)_3$, $CDCl_3$, 7 days; (ii) 65 °C, 2 days; (iii) $PPh_{3-x}(py)_x$, NH_4PF_6, acetone, 20 h; (iv) $PPh_{3-x}(py)_x$, C_6H_6, 2 h; (v) Δ, C_6H_6, 2 h; (vi) NH_4PF_6, acetone, 1 h; (vii) $CDCl_3$ or CD_2Cl_2.

septet for the PF_6^-. The spectrum of **1c** is identical to that seen in the in situ reaction (above); hence, **1c′** is formulated as the chloride analogue of **1c**. The high-field triplets (P_X) of the $PPh_{3-x}(py)_x$ ligands result because of the formation of four-membered chelate rings[15] and are farther upfield of the signals seen for *P*,*N*-coordinated $PPh_{3-x}(py)_x$ complexes;[4] the low-field doublets (P_A) result from the two PPh_3 ligands. The ^1H NMR ($CDCl_3$) spectra (Table 4, Supporting Information) showed multiple peaks in the phenyl region. The $PPh(py)_2$ complex **1b** showed one H6 signal[16] integrating for two protons, while the $P(py)_3$ complex **1c** showed two H6 signals integrating in a 1:2 ratio, indicating the complexes contain two equivalent pyridyl groups. These solution NMR data are consistent with the X-ray crystal structures, which revealed a strained coordination mode around the phosphorus of the 2-pyridylphosphine ligand.

Complexes **1b** and **1c** have the "same" structures, and an ORTEP plot of **1b** is shown in Figure 2. The 2-pyridylphosphine ligands bind via the P and two pyridyl-N atoms, forming two four-membered rings, causing a distorted octahedral geometry as shown, for example, by the Cl(1)−Ru−P(1) angles and the N(1)−Ru−N(2) angles (Table 2). There are minimal differences between cooresponding bond lengths of **1b** and **1c** (Table 2). The Ru−P bond lengths fall within the range typical of Ru(II) phosphine complexes.[17] The Ru−Cl bond lengths, like the Ru−N bonds, are identical between **1b** and **1c**, while within either **1b** or **1c** the Ru−N bond lengths are marginally different, indicating the $PPh_{3-x}(py)_x$ ($x = 2, 3$) ligands are bound essentially symmetrically.

Corresponding angles of the two four-membered rings in any one complex are essentially identical, as are the corresponding ring angles found between **1b** and **1c**. The P−C−N angles within the four-membered rings in **1c** (100.8(2)°) are compressed compared to those found in free $P(py)_3$ (average 117.2°).[18] The

(15) Garrou, P. E. *Chem. Rev.* **1981**, *81*, 229.

(16) The H6 protons (adjacent to N in the 2-pyridyl group) generally appear downfield from other protons in the phenyl region (NMR spectra) and have a distinctive identifiable pattern, appearing as approximate doublets (actually multiplets). (a) Jackobsen, H. J. *J. Mol. Spectrosc.* **1970**, *34*, 245. (b) Griffin, G. E.; Thomas, W. A. *J. Chem. Soc. (B)* **1970**, 477.

(17) Jessop, P. G.; Rettig, S. J.; Lee, C.-L.; James, B. R. *Inorg. Chem.* **1991**, *30*, 4617.

(18) Keene, F. R.; Snow, M. R.; Tiekink, E. R. T. *Acta Crystallogr., Sect. C* **1988**, *44*, 757.

Table 3. $^{31}P\{^1H\}$ NMR Chemical Shifts for Neutral and Cationic Ruthenium $PPh_{3-x}(py)_x$ ($x = 1, 2, 3$) Complexes

		δ (ppm)			J (Hz)		
neutral complexes (AMX spin systems)	solvent	P_A	P_M	P_X	$^2J_{AM}$	$^2J_{AX}$	$^2J_{MX}$
trans-$RuCl_2$(dppb)(PPh_2(py)) (**2a**)	$CDCl_3$	43.3	25.2	−22.5	36.7	27.1	324
trans-$RuCl_2$(dppb)(PPh(py)$_2$) (**2b**)	$CDCl_3$	42.5	26.5	−20.5	36.1	26.4	321
trans-$RuCl_2$(dppb)(P(py)$_3$) (**2c**)	$CDCl_3$	42.0	26.8	−18.4	36.3	26.3	316
cis-$RuCl_2$(dppb)(PPh_2(py)) (**3a**)	$CDCl_3$	47.8	36.5	−20.9	34.6	26.3	27.4
cis-$RuCl_2$(dppb)(PPh(py)$_2$) (**3b**)[a]	CD_2Cl_2	47.5	37.1	−13.8	34.9	26.2	25.9
	CD_2Cl_2	48.9	39.3	−14.3	32.9	*b*	27.6
cis-$RuCl_2$(dppb)(P(py)$_3$) (**3c**)	$CDCl_3$	49.5	39.4	−7.97	33.8	25.3	26.4

		δ (ppm)		
cationic complexes[c] (A_2X spin systems)	solvent	P_A	P_X	$^2J_{AX}$
[RuCl(PPh_3)$_2$(P(py)$_3$)]Cl (**1c′**)[d]	$CDCl_3$	44.0	−46.7	25.5
[RuCl(PPh_3)$_2$(PPh(py)$_2$)]PF_6 (**1b**)	$CDCl_3$	43.6	−45.6	25.6
[RuCl(PPh_3)$_2$(P(py)$_3$)]PF_6 (**1c**)	$CDCl_3$	43.9	−46.5	25.5
[RuCl(dppb)(PPh(py)$_2$)]Cl[e]	$CDCl_3$	47.0	−36.6	24.6
	CD_2Cl_2	47.4	−36.6	24.4
	CD_3OD	47.2	−35.1	24.5
[RuCl(dppb)(PPh(py)$_2$)]PF_6 (**4b**)	$CDCl_3$	46.8	−36.8	24.3
[RuCl(dppb)(P(py)$_3$)]Cl[f]	$CDCl_3$	46.7	−41.2	23.6
	CD_3OD	47.1	−38.7	23.9
[RuCl(dppb)(P(py)$_3$)]PF_6 (**4c**)	$CDCl_3$	46.7	−40.9	23.9

[a] Mixture of two diastereomers. [b] P_A and P_X signals are broad; coupling is not resolved. [c] The PF_6^- anion is observed as a septet at δ −144 ($^1J_{PF}$ = 713 Hz). [d] In situ. [e] In equilbrium with **3b** (CD_2Cl_2). [f] In equilbrium with **3c** ($CDCl_3$).

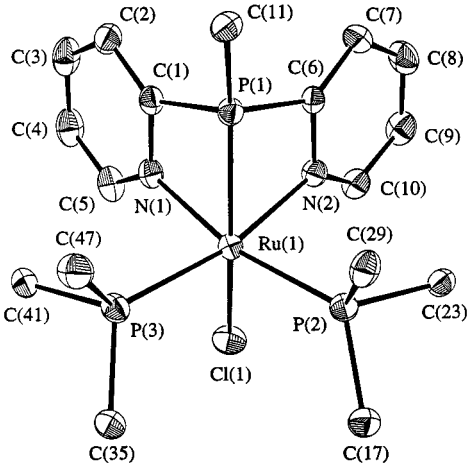

Figure 2. ORTEP plot (33% probability thermal ellipsoids) of cation in **1b**, showing atom labeling (labeling for **1c** is the same). Phenyl groups have been omitted for clarity.

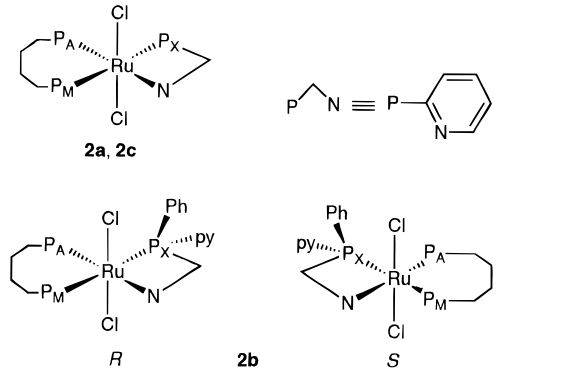

Figure 3. Structures of *trans*-$RuCl_2$(dppb)($PPh_{3-x}(py)_x$) ($x = 1$ (**2a**), 2 (**2b**), 3 (**2c**)). Phosphorus labels correspond to chemical shifts given in Table 3.

P,N,N′-coordination mode in **1c** also shows strain around the P atom: the two coordinated pyridyl groups are pulled closer toward each other in comparison to the situation in the free ligand [the C(1)−P(1)−C(6) angle (96.6(1)°) is compressed, while the C(6)−P(1)−C(11) (111.6(1)°) and C(1)−P(1)−C(11) (110.9(1)°) angles are expanded, compared to an average of 101.9° in free P(py)$_3$].[18] The bond lengths within P(py)$_3$ do not change upon its coordination. Although the crystal structure of PPh(py)$_2$ has not been reported, a similar strain is expected in the PPh(py)$_2$ complex **1b**.

When equivalent amounts of $RuCl_2$(dppb)(PPh_3) and $PPh_{3-x}(py)_x$ ($x = 1-3$) were reacted, *trans*-$RuCl_2$(dppb)(PPh_{3-x}(py)$_x$) ($x = 1$ (**2a**), 2 (**2b**), 3 (**2c**)) were isolated in 83−93% yields. The structures, including assignments for the $^{31}P\{^1H\}$ NMR signals (Table 3), are shown in Figure 3. The ^1H NMR spectra (Table 4, Supporting Information) contain multiple peaks in the phenyl region, as well as signals in the methylene region for the dppb backbone, reflecting the planar symmetry. Thus, for the PPh_2(py) (**2a**) and P(py)$_3$ (**2c**) complexes, three signals are seen for the dppb methylenes in a 1:1:2 integration ratio. For the PPh(py)$_2$ complex (**2b**), the planar symmetry is interrupted because of the chirality of the PPh(py)$_2$ ligand when it is *P,N*-coordinated. While one pyridyl group is coordinated, the second projects to one side of the plane, with the phenyl group projecting to the other. This is seen in the dppb methylene signals, which appear in a 1:2:1:4 integration ratio. Complex **2b** is, therefore, isolated as a mixture of enantiomers.

The *trans*-$RuCl_2$(dppb)($PPh_{3-x}(py)_x$) complexes (**2a**−**c**), when heated in solution, isomerize to isolable, yellow *cis*-$RuCl_2$(dppb)($PPh_{3-x}(py)_x$) solids (**3a**−**c**) (89−93% yields). The neutral *cis* complexes lose chloride in solution (Figure 4), the extent of dissociation being solvent-dependent. In the case of **3b** and **3c**, *P,N,N′*-coordinated cationic complexes (Figure 4) are formed, and these were isolated as their PF_6^- salts by reaction of **3b** or **3c** with 1 equiv of NH_4PF_6 in acetone to give [RuCl(dppb)($PPh_{3-x}(py)_x$)]PF_6 ($x = 2$ (**4b**), 3 (**4c**)). Prior to discussion of the equilibria shown in Figure 4 and the characterization of the neutral *cis* species, complexes **4b** and **4c** are considered.

Complexes **4b** and **4c** are dppb analogues of [RuCl(PPh_3)$_2$($PPh_{3-x}(py)_x$)]PF_6 ($x = 2$ (**1b**), 3 (**1c**)). The $^{31}P\{^1H\}$ NMR spectra (Table 3) are similar to those of **1b** and **1c** and consist of A_2X patterns for the cations. The ^1H NMR spectra (Table 4, Supporting Information) are also similar to those of **1b** and **1c**. From integration of the H6-py signals versus those

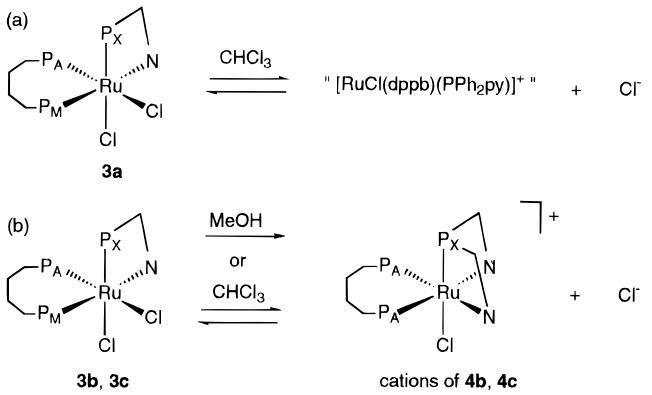

Figure 4. Dissociation of a chloride from *cis*-$RuCl_2$(dppb)(PPh_{3-x}-$(py)_x$) (x = 1 (**3a**), 2 (**3b**), 3 (**3c**)). Phosphorus labels correspond to chemical shifts reported in Table 3. Complexes **3a** and **3c** are chiral at the metal center, and only the Δ isomer is shown, while **3b** is chiral at both the P of the $PPh(py)_2$ and the metal center.

of the dppb methylenes, the two pyridyl groups of **4b** are equivalent (coordinated), while **4c** contains two equivalent (coordinated) and one inequivalent (uncoordinated) pyridyl group. Four signals, each integrating for two protons, are seen for the dppb methylene protons. Complexes **4b** and **4c** are 1:1 electrolytes in CH_3NO_2.

For the $PPh_2(py)$ complex **3a**, the $^{31}P\{^1H\}$ NMR ($CDCl_3$) spectrum (Table 3) consists of an AMX pattern (*cis* $^2J_{AX}$, $^2J_{AM}$, $^2J_{MX}$), consistent with its neutral formulation (Figure 4). Furthermore, the dppb methylenes give rise to seven ^1H NMR signals (Table 4, Supporting Information) because of the complex's asymmetry. In the $^{31}P\{^1H\}$ NMR spectrum at 20 °C, the low-field signal (P_A) of the phosphorus *trans* to chloride is broad, while at 45 °C the signal begins to resolve into a doublet of doublets; the broadness is attributed to reversible chloride dissociation (Figure 4). Further evidence from conductivity data shows that the complex is a 1:1 conductor in CH_3NO_2.

For the $PPh(py)_2$ complex **3b**, the $^{31}P\{^1H\}$ NMR ($CDCl_3$) spectrum shows loss of chloride and formation of the cationic *P,N,N′* complex. The spectrum is identical to that of **4b** (discussed above). When the solvent is changed to CD_2Cl_2, which does not support the formation of ions as well as $CDCl_3$, the signals for neutral **3b** are seen also as two AMX patterns. Two patterns appear because **3b** occurs as a mixture of two diastereomeric pairs due to the chirality at the metal center and the chirality of the *P,N*-coordinated $PPh(py)_2$. One of the diastereomers probably undergoes reversible chloride dissociation on the NMR time scale, as two of the signals appear broad.

Further evidence for the presence of the neutral *cis* complex is seen when comparing the UV−visible spectrum of **3b** in $CHCl_3$ with that of the PF_6^- salt **4b** in $CHCl_3$, which suggests that **3b** is not entirely dissociated to the cationic *P,N,N′* complex. In MeOH, **3b** dissociates completely to give the cation, and the UV−visible spectra of **3b** and **4b** are essentially identical. Similar UV−visible data are obtained with the $P(py)_3$ analogue **3c** (below).

For the $P(py)_3$ complex **3c**, the $^{31}P\{^1H\}$ NMR ($CDCl_3$) spectrum shows both an AMX pattern for the neutral *cis* complex and an A_2X pattern for the cationic *P,N,N′* species (identical to that of **4c**). As well, the ^1H NMR ($CDCl_3$) spectrum contains four dppb methylene signals, attributable to the *P,N,N′* cationic species (as in **4c**), and six methylene signals for the neutral species **3c**, similar to those seen for **3a**. Furthermore, the $^{31}P\{^1H\}$ NMR (CD_3OD) spectrum of **3c** contains only the A_2X pattern of the cationic *P,N,N′* species;

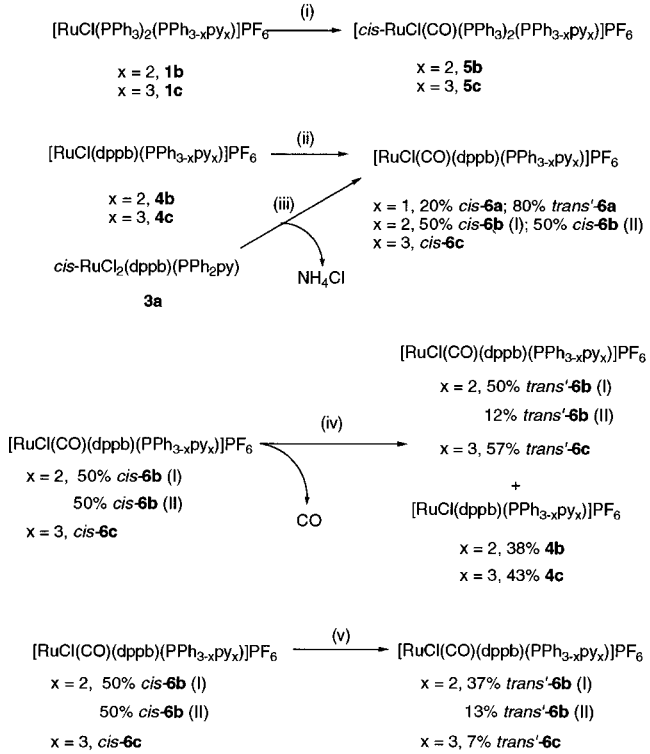

Figure 5. Summary of syntheses and reactivities of carbonyl compounds. Conditions: (i) CO (1 atm) (1 equiv for x = 2), CH_2Cl_2 or acetone; (ii) CO (1 atm), CH_2Cl_2, 1 h; (iii) NH_4PF_6, CO (1 atm), acetone, 21 h; (iv) Δ, $CHCl_3$, Ar (1 atm), 24 h for x = 3, 16 h for x = 2; (v) CO (1 atm), CH_2Cl_2, 6 days. Percentages reported are relative compositions of isolated products. **I** and **II** represent diastereomers.

when the complex is isolated from the CD_3OD solution and the spectrum is then remeasured in $CDCl_3$, both the neutral and cationic species (in about a 1:1 ratio) are again observed, showing that chloride loss is reversible.

The reversible chloride equilibria described above provide insight into the reasons why the in situ complex [$RuCl(PPh_3)_2$-$(P(py)_3)$]Cl (**1c′**) could not be isolated. Addition of ether or hexanes (used in attempts to isolate **1c′** from $CHCl_3$) presumably causes reassociation of the chloride ion; however, the isolated product is not a pure neutral *cis* species analogous to **3c**, as evidenced by the $^{31}P\{^1H\}$ NMR spectrum. The chelating dppb ligand in **3c**, compared to the two PPh_3 ligands in **1a**, perhaps limits the number of sites where free chloride ion can reassociate. Hence, **3c** is stable to chloride dissociation during the workup procedure, while **1c′** is unstable and several complexes are isolated.

Reactivity of Complexes with the *P,N,N′*-Coordination Mode: Carbonyl Derivatives. The *P,N,N′*-coordinated 2-pyridylphosphine complexes described here have the potential of becoming coordinatively unsaturated via dissociation of one of the pyridyl groups, because of the strain observed in this type of coordination. This has potential for catalysis, and so the reactivity with small molecules was investigated. Complexes **1b**, **1c, 3a**, **4b**, and **4c** did not react with H_2 or O_2 (in $CDCl_3$ at ambient conditions over 24 h); similarly, **4b** was unreactive toward N_2 and **3c** toward H_2. However, reactions do occur with CO under comparable conditions.

Figure 5 (i−iii) summarizes the reactivity of the complexes with CO. Orange solutions of [$RuCl(PPh_3)_2(PPh_{3-x}(py)_x)$]$PF_6$ (x = 2, **1b**; 3, **1c**) in acetone or CH_2Cl_2 turned yellow upon exposure to CO. A gas uptake experiment with **1c** in CH_2Cl_2 (the technique has been described elsewhere)[19] under 1 atm of CO showed that only 1 equiv of CO was consumed in 1 h.

Table 5. $^{31}P\{^1H\}$ NMR ($CDCl_3$) Chemical Shifts and Carbonyl Stretching Frequencies for Ruthenium $PPh_{3-x}(py)_x$ ($x = 1-3$) Carbonyl Complexes [a]

		δ (ppm)			J (Hz)			
complex	spin system	P_A	P_M or P_B	P_X	$^2J_{AX}$	$^2J_{AM}$ or $^2J_{AB}$	$^2J_{MX}$ or $^2J_{BX}$	ν_{CO}[b] (cm^{-1})
[*cis*-RuCl(CO)$(PPh_3)_2(PPh_{3-x}(py)_x)$]$PF_6$								
$x = 2$, **5b**	ABX	36.9	33.9	−14.4	21.2	296	20.0	1953
$x = 3$, **5c**	A_2X	35.9		−16.2	20.8			1961
[*cis*-RuCl(CO)(dppb)$(PPh_{3-x}(py)_x)$]X								
$x = 1$; X = Cl	AMX	36.9	18.6	−17.2	21.8	33.1	26.4	
$x = 1$; X = PF_6, *cis*-**6a**[c]	AMX	36.4	18.7	−17.8	20.9	33.3	26.0	2004
$x = 2$; X = PF_6, *cis*-**6b (I)**[d]	AMX	39.7	18.1	−14.5	21.1	33.4	27.1	2007
cis-**6b (II)**[d]	AMX	33.5	23.0	−7.39	24.1	33.3	24.0	2018
$x = 3$; X = PF_6, *cis*-**6c**	AMX	32.6	21.7	−6.03	22.5	33.2	25.3	2021
[*trans*-RuCl(CO)(dppb)$(PPh_{3-x}(py)_x)$]X								
$x = 1$; X = Cl	AMX	36.4	20.3	−30.4	20.3	28.5	298	
$x = 1$; X = PF_6, *trans′*-**6a**	AMX	36.4	20.1	−30.6	20.3	28.9	298	1961
$x = 2$; X = PF_6, *trans′*-**6b (I)**[e]	AMX	37.7	23.9	−24.3	23.0	29.0	298	1969
trans′-**6b (II)**[e]	AMX	33.4	23.7	−28.0	21.6	28.8	291	
$x = 3$; X = PF_6, *trans′*-**6c**	AMX	33.9	25.4	−22.7	22.0	28.8	288	1973

[a] ~20 °C in $CDCl_3$: PF_6^- −144 ppm (septet), $^1J_{PF} = 713$ Hz. [b] Nujol mull/KBr plates. Where not reported, ν(CO) values were either not measured or unobserved. [c] **6a** isolated as mixture of *cis* and *trans′* isomers. [d] *Cis*-**6b** is a 50:50 mixture of two diastereomers, labeled **I** and **II**. [e] Produced from isomerization *cis*-**6b** (**I** and **II**), respectively.

Complex **1b** was reacted with only 1 equiv of CO because of the formation of, presumably, dicarbonyl complexes, which were observed in small amounts in the $^{31}P\{^1H\}$ NMR ($CDCl_3$) spectrum of **1b** under 1 atm of CO. The second CO is believed to displace a PPh_3 ligand, as the $^{31}P\{^1H\}$ NMR spectrum showed the presence of free PPh_3. The products isolated are *cis*-[RuCl(CO)$(PPh_3)_2(PPh_{3-x}(py)_x)$]$PF_6$ ($x = 2$, **5b**; 3, **5c**), *cis* referring to the disposition of the CO and Cl ligands.

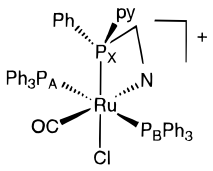

5b

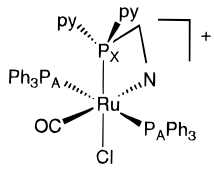

5c

The $^{31}P\{^1H\}$ NMR spectra of **5b** and **5c** (Table 5) are consistent with the structures shown. Compound **5b** is isolated as a racemate, the P atom of the coordinated $PPh(py)_2$ ligand being chiral. The high-field signal (P_X) is assigned to the *P,N*-coordinated $PPh(py)_2$ ligand; an AB pattern is assigned to the two PPh_3 ligands, which are not equivalent because of the chirality. The spectrum is consistent with *trans* PPh_3 ligands with a mutually *cis* $PPh(py)_2$ ligand. The simpler A_2X spectrum was seen for **5c**, where the two PPh_3 ligands are equivalent.

The arrangement of the Cl and CO ligands is based on the ν(CO) IR data. The lower values (Table 5), relative to those of the [*cis*-RuCl(CO)(dppb)$(PPh_{3-x}(py)_x)$]PF_6 complexes ($x =$ 2, *cis*-**6b**; 3, *cis*-**6c**), where the CO ligand is *trans* to phosphorus (see below), suggest that the CO in **5b** and **5c** is *trans* to the N atom of the coordinated pyridyl groups.

A small amount of a second species is evidenced in the $^{31}P\{^1H\}$ NMR spectrum of **5b**. (AMX (ppm): $P_A = 35.7$; $P_M = 21.7$; $P_X = -34.9$; $^2J_{AX} = 29.1$; $^2J_{AM} = 21.3$; $^2J_{MX} = 313$ Hz.) This complex is tentatively assigned a structure similar to that of the dppb complexes *trans′*-**6a**−**c** described below, with the two PPh_3 ligands replacing the dppb.

The dppb analogues of **1b** and **1c**, namely [RuCl(dppb)$(PPh_{3-x}(py)_x)$]PF_6 ($x = 2$, **4b**; 3, **4c**), also react with 1 atm of CO to produce [*cis*-RuCl(CO)(dppb)$(PPh_{3-x}(py)_x)$]PF_6 ($x = 2$, *cis*-**6b**; 3, *cis*-**6c**). Both complexes were isolated with ether solvates, the amount being determined by integration of the ^1H NMR spectra. An attempt to remove the Et_2O solvate from *cis*-**6b** by heating the complex under vacuum (78 °C for 4 days) caused a 5% conversion back to the starting material, **4b**. Thus, CO loss can occur in the solid state, although slowly. The reversibility of these CO reactions is discussed below.

The structures of *cis*-**6b** and *cis*-**6c** are assigned on the basis of the observed spectroscopic data. The $^{31}P\{^1H\}$ NMR data are consistent with all *cis* phosphorus atoms, as well as a *P,N*-coordinated $PPh_{3-x}(py)_x$ ligand. The P_X signals are assigned to the $PPh_{3-x}(py)_x$ ($x = 2$, 3) ligands, while the P_A and P_M signals (Table 5) are assigned to the dppb ligands. The ^1H NMR spectra (e.g., eight signals for the eight dppb methylene protons in *cis*-**6c**, Table 6 (Supporting Information)) confirm the asymmetry of the complexes. For both complexes, the CO and Cl are mutually *cis*, and the relative positions with respect to the other ligands can be assigned after further consideration. Studies from this group have established an inverse relation between Ru(II)−PPh_3 bond lengths and the corresponding δ_P shifts,[17] and this correlation has been extended to complexes containing dppb.[20] After consideration of the *trans influence* of Cl and CO[21] and their effects on Ru−P bond lengths, as well as the differences between the δ_P values observed for the carbonyl complexes and the neutral *cis*-dichloro complexes **3a**−**c**, the relative positions of the CO and Cl can be determined.

The two possible structures for the carbonyl compounds *cis*-**6b** and *cis*-**6c** are shown in Figure 6 (labeled **A** and **B**), along with the structure for the analogous dichloro complexes. As an example, the δ_P data for *cis*-**6c** and **3c** are given, as well as the absolute differences in the chemical shifts between the two compounds. If the CO is trans to a P atom of dppb (Figure 6, structure **A**), the Ru−P bond length is expected to be longer in the carbonyl complex than in the neutral chloro complex (*trans influence* of Cl vs CO). Therefore, the P_A signal for the neutral chloro complex should shift upfield in the carbonyl complex, with the other signals remaining relatively unchanged as they are *trans* to identical ligands in both complexes. This is, in fact, observed: the P_A signal in **3c** shifts upfield by 27.8 ppm in *cis*-**6c** (now the P_M signal), the other signals shifting by small amounts. If the CO were *trans* to the P atom of the $P(py)_3$ ligand (Figure 6, structure **B**), a larger difference in the chemical

(19) James, B. R.; Mahajan, D. *Isr. J. Chem.* **1977**, *15*, 214.

(20) (a) MacFarlane, K. S.; Joshi, A. M.; Rettig, S. J.; James, B. R. *Inorg. Chem.* **1996**, *35*, 7304. (b) MacFarlane, K. S. Ph.D. Thesis, University of British Columbia, 1995.

(21) Huheey, J. E. *Inorganic Chemistry*, 3rd ed.; Harper & Row: New York, 1983; p 542.

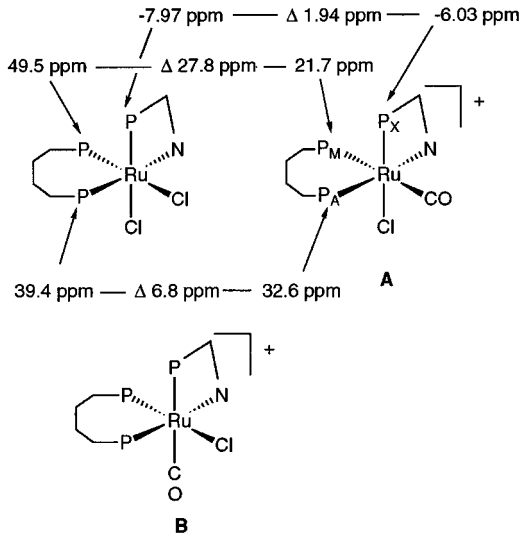

Figure 6. Possible structures for [*cis*-RuCl(CO)(dppb)($PPh_{3-x}(py)_x$)]-PF_6 ($x = 2$, *cis*-**6b**; 3, *cis*-**6c**) and the structure of the *cis* neutral dichloro complexes **3a**−**c**. Chemical shifts given are for the $P(py)_3$ complexes *cis*-**6c** and *cis*-**3c**.

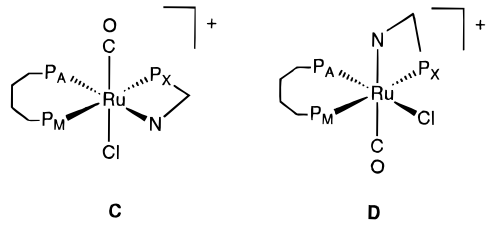

Figure 7. Possible structures for [*trans*′-RuCl(CO)(dppb)($PPh_{3-x}(py)_x$)]-PF_6 ($x = 1$, *trans*′-**6a**; 2, *trans*′-**6b**; 3, *trans*′-**6c**). Phosphorus labels correspond to those reported in Table 5.

shifts of the P_X signals would be expected. Thus, the CO is almost certainly *trans* to the dppb, as in structure **A**.

The *P*,*N*-coordinated $PPh(py)_2$ complex, *cis*-**6b**, is isolated as a mixture (50:50) of two diastereomers (with their corresponding enantiomers), labeled *cis*-**6b** (**I**) and *cis*-**6b** (**II**) in Table 5 and Table 6 (Supporting Information), the chirality occurring at the coordinated P atom of $PPh(py)_2$ and at the metal center because of the presence of two chelate rings. The ν(CO) and ^{1}H NMR data were correlated with the $^{31}P\{^1H\}$ NMR data, based on the isomerizations described below, and this allows assignment of NMR signals and ν(CO) values to specific diastereomers.

To complete the 2-pyridylphosphine ligand series of *cis*-chloro(carbonyl) complexes, the reaction of *cis*-$RuCl_2$(dppb)-(PPh_2(py)) (**3a**) with CO (1 atm) and 1 equiv of NH_4PF_6 gave a mixture of 20% *cis*- and 80% *trans*′-[RuCl(CO)(dppb)(PPh_2-(py))]PF_6 (**6a**). Their structures are analogous to the corresponding structures of *cis*-**6c** (Figure 6, **A**) and *trans*′-**6c** (Figure 7, **C** or **D** see below), respectively. The in situ reaction of **3a** with CO but without added NH_4PF_6 in $CDCl_3$ was followed by $^{31}P\{^1H\}$ NMR spectroscopy. *Cis* and *trans*′ complexes analogous to **6a** were observed, but other reactions occurred, as evidenced by the presence of other peaks in the $^{31}P\{^1H\}$ NMR spectrum, including those for free dppb (−16.2 ppm) and PPh_2-(py) (−3.95 ppm). The isolated mixture of *cis*/*trans*′-**6a** was converted mainly to the *trans*′-isomer by heating a $CDCl_3$ NMR sample of the mixture at 50 °C for 24 h. In summary, complexes with the *P*,*N*,*N*′-coordinated 2-pyridylphosphines undergo reactions with CO, with the displacement of one coordinated pyridyl group, to form *P*,*N*-coordinated complexes. No evidence was found for the displacement of the second pyridyl group, suggesting that the *P*,*N*-coordination mode is stable to displacement by CO. The reason may be that Ru(II) is incapable of supporting three phosphine and two CO π-acceptor ligands, as evident in $RuCl_2(CO)_2(PPh_2(py))$, where CO does not displace the pyridyl group of the *P*,*N*-coordinated PPh_2(py).[4a]

It should be noted that complexes **1b** and **1c** do catalyze the hydrogenation of imines in MeOH solution at 20 °C under 500 psi H_2; e.g., 0.1 M $PhCH_2N{=}CHPh$ undergoes 53% conversion to dibenzylamine in 3 h using 0.75 mM [$RuCl(PPh_3)_2$(*P*,*N*,*N*′-$PPh(py)_2$)] (**1b**).[22] This implies that the complexes (or an imine derivative) are capable of activating H_2 at elevated pressure. Incorporation of an N-donor ligand at Ru(II) (sometimes as a P−N chelate) has been found recently to generate active catalysts for hydrogen transfer hydrogenation (from 2-propanol or formic acid) of imines and ketones.[23]

Isomerization of, and CO Loss from, the Carbonyls. The carbonyl complexes *cis*-**6b** and *cis*-**6c** (Figure 6, **A**) can isomerize in solution (see Figure 5, iv and v). These isomerizations were performed first in refluxing $CHCl_3$ under 1 atm of Ar, and second at ∼20 °C in CH_2Cl_2 under 1 atm of CO. After certain times, the products were isolated by removing the solvent under vacuum and were then analyzed by NMR and IR spectroscopies. Relative amounts of compounds were determined by integration of the H6 proton signals, after correlating the relative amounts with the IR and $^{31}P\{^1H\}$ NMR spectra. Under the first set of conditions, *cis*-**6b** and *cis*-**6c** undergo isomerization to **C** or **D**, for convenience called *trans*′ products, implying *trans* P atoms (Figure 7, see below), and also generate via loss of CO some **4b** and **4c**, respectively.

In CH_2Cl_2 under CO at ∼20 °C, ∼7% of *cis*-**6c** is converted to *trans*′-**6c** after 6 days; after 20 days, the conversion was 12%. There was no loss of CO from the sample under these conditions. Similarly, under CO, a slow isomerization of *cis*-**6b** occurred; in this case, the two diastereomers *cis*-**6b** (**I**) and *cis*-**6b** (**II**) isomerized at different rates, allowing for correlation of the ν(CO) values and ^{1}H NMR signals with the $^{31}P\{^1H\}$ NMR data, as well as allowing for the correlation of which *cis* diastereomer produced which *trans* diastereomer (Figure 5, v).

The possible structures for the *trans*′ isomerization products are shown in Figure 7, labeled **C** and **D**. The $^{31}P\{^1H\}$ NMR data are consistent with *P*,*N*-coordinated $PPh_{3-x}(py)_x$ (P_X), with *cis* (P_A) and *trans* (P_B) nuclei of dppb. The ν(CO) values are lower than those seen for the corresponding *cis* complexes (above), which is consistent with the CO being *trans* to either Cl or N, versus P in the *cis* complexes. Thus, no definite assignments for the structures of the isomerization products are made. With the *cis* complexes, the relative positions of the dppb and the *P*,*N*-chelate were fixed, leaving only the assignment of the Cl and CO positions. With the isomerization products, the relative positions of dppb and only the P atom of the *P*,*N*-chelate are known, leaving three positions which need to be assigned.

π-Acceptor Abilities of the $PPh_{3-x}(py)_x$ Ligands ($x = 1-3$). Increased incorporation of the electron-withdrawing 2-pyridyl groups[24] in the $PPh_{3-x}(py)_x$ ligands decreases the σ-donating ability in the order $x = 1 > x = 2 > x = 3$. Correspondingly, the π-acceptor ability should be enhanced in the order $x = 3 > x = 2 > x = 1$, and the ν(CO) values for the *cis* and *trans*′ carbonyl complexes (**6a**−**c**) validate this, the carbonyl stretches (Table 5) increasing in energy in the order **6a** ($PPh_2(py)$) < **6b** ($PPh(py)_2$) < **6c** ($P(py)_3$). The enhanced π-acceptor ability as the ligand is changed from $PPh_2(py)$ to $P(py)_3$ increases the

(22) Schutte, R. P. Ph.D. Thesis, University of British Columbia, 1995.
(23) Noyori, R.; Hashiguchi, S. *Acc. Chem. Res.* **1997**, *30*, 97.
(24) Perrin, D. D.; Dempsey, B.; Serjeant, E. P. *pK_a Prediction for Organic Acids and Bases*; Chapman and Hall: London, 1981; p 119.

competition for back donation from the Ru(II), which manifests itself in the strengthening of the CO bond. The trend is also consistent with $PPh_2(py)$ being a better π-acceptor than PPh_3, as determined from the ν(CO) values for $Ni(CO)_2(PPh_3)_2$ and $Ni(CO)_2(PPh_2(py))_2$.[2a]

Summary

Several complexes were synthesized containing the previously uncharacterized *P*,*N*,*N*′-coordination mode for 2-pyridylphosphine ligands. The *P*,*N*,*N*′-coordination mode is highly strained, based on the observed angles in the crystal structure of $[RuCl(PPh_3)_2(P(py)_3)]PF_6$, and leads to reactivity to relieve the strain. The *P*,*N*,*N*′-coordinated 2-pyridylphosphine complexes are capable of undergoing reversible reactions with Cl^- and CO, which displace a coordinated pyridyl group. Finally, the carbonyl compounds characterized allow for a relative ordering of π-acceptor ability to be established for the 2-pyridylphosphine ligands.

Acknowledgment. Financial support from the Natural Sciences and Engineering Research Council of Canada is gratefully acknowledged as are loans of ruthenium from Johnson Matthey PLC and Colonial Metals Inc.

Supporting Information Available: Tables 4 and 6, giving the ^{1}H NMR data for ruthenium $PPh_{3-x}(py)_x$ ($x = 1-3$) and ruthenium $PPh_{3-x}(py)_x$ ($x = 1-3$) carbonyl complexes (3 pages). X-ray crystallographic files, in CIF format, for $([RuCl(PPh_3)_2(P,N,N'\text{-}PPh(py)_2)]PF_6$ and $RuCl(PPh_3)_2(P,N,N'\text{-}P(py)_3)]PF_6$ are available on the Internet only. Access and ordering information is given on any current masthead page.

IC970835J